Prediction of effective heat transfer performance of metal foam heat exchangers

Sahan Trushad Wickramasooriya Kuruneru[1,a], Emilie Sauret[1,b*], Suvash Chandra Saha[1,c], YuanTong Gu[1,d]

[1]School of Chemistry, Physics & Mechanical Engineering, Queensland University of Technology, Brisbane, Australia

[a]sahan.kuruneru@hdr.qut.edu.au, [b]emilie.sauret@qut.edu.au, [c]suvash.saha@qut.edu.au, [d]yuantong.gu@qut.edu.au

Keywords: metal foam heat exchanger, Weaire-Phelan, heat transfer

Abstract.

A numerical investigation of heat transfer performance of metal foams is conducted to predict the local temperature distribution of the flow and metal foam ligaments. This examination will serve as a stepping stone to better optimize metal foam heat exchanger designs. An idealized Weaire-Phelan metal foam model is used in this investigation. The magnitudes of local temperature hotspots differ due to the foam's geometric profile, namely the foam fibre thickness. The heat transfer characteristics of the fouling zone is predicted based on the foam wall's temperature distribution hot spots.

Introduction

Heat exchangers are omnipresent in an array of applications such as power stations, electronics cooling, and HVAC&R. The global heat exchanger market is projected to reach US $78.16 billion by 2020 [1]; a major challenge lies in developing more innovative, economical, and effective heat transfer technologies. One such material that is gaining extensive popularity is metal foams. Open-cell metal foam, a class of highly porous material, exhibits superior qualities such as high thermal conductivity, high surface area to volume ratio, low weight [2]. The stochastic orientation of these fibrous structures enhance turbulence and fluid mixing. This trait makes metal foams an attractive material in a number of applications such as compact heat exchangers.

Metal foam heat exchangers are shown to have superior heat transfer performance as compared to that of a conventional finned tube heat exchanger [3]. A study by Bai & Chung [4] has found that a foam filled tube has a heat transfer rate two orders of magnitude higher than an open tube macro channel.A copper foam heat exchanger based on 45 pores per inch (PPI) is shown to exhibit a higher heat transfer rate than a bare tube bundle by a factor of six at the same fan power [5].A study by Mahdi et al. [6] experimentally concluded that aluminium-foam Central Processing Unit (CPU) heat exchangers yield 70% lower thermal resistance compared to fin-based CPU heat exchangers. However, this was based on natural convection and single phase flows (hot air) and the effects of dust-laden flows on the overall thermal resistance on both aluminium and copper foams hasn't been investigated. Seyf & Layeghi [7]conducted a comparative assessment of the heat transfer performance of a fin heat sink with and without metal foams. In some cases, an increase in Reynolds number and decrease in foam porosity, results in a 400 % increase in the Nusselt number.

All of these studies is confined to *single-phase flows*; however, many applications such as heat exchangers are based on *multiphase flows*, such as, particle-laden gas flows in air cooled heat exchangers. Kuruneru et al. [8] examined poly-disperse particulate fouling in an idealized metal foam heat exchanger but the study is restricted to simple 2D isotropic configurations and the effects on heat transfer was not considered. The existing literature is devoid of examining the potential impact particulate fouling may have on the effective thermal performance of a metal foam heat exchanger.

The goal of this work is to examine the temperature distribution of several metal foam specimensand predict the heat transfer characteristics and temperature hotspotsthat are linked to particle deposition areas. ANSYS Fluent will be used to perform the pore-level numerical investigation of an idealized Weaire-Phelan (WP) unit cell.

Numerical Model and Computational Domain

The transport of mass, momentum, and energy of incompressible Newtonian fluid at the pore level is governed by the Navier-Stokes equations and is shown in equations 1-3[9]

$$\frac{\partial}{\partial x_i}\rho_f u_i = 0 \tag{1}$$

$$\frac{\partial}{\partial x_i}\left(\rho_f u_j u_i\right) = -\frac{\partial P}{\partial x_i} + \frac{\partial}{\partial x_i}\left(\mu_f \frac{\partial u_i}{\partial x_j}\right) \tag{2}$$

$$\frac{\partial}{\partial x_i}\left(\rho_f u_i c_p T\right) = \frac{\partial}{\partial x_i}\left(\lambda \frac{\partial T}{\partial x_i}\right) \tag{3}$$

where fluid density is denoted as ρ_f, fluid velocity u, pressure P, dynamic viscosity μ_f, specific heat capacity c_p, temperature T, and air thermal conductivity λ.The computation domain and boundary conditions are shown in Fig.1.

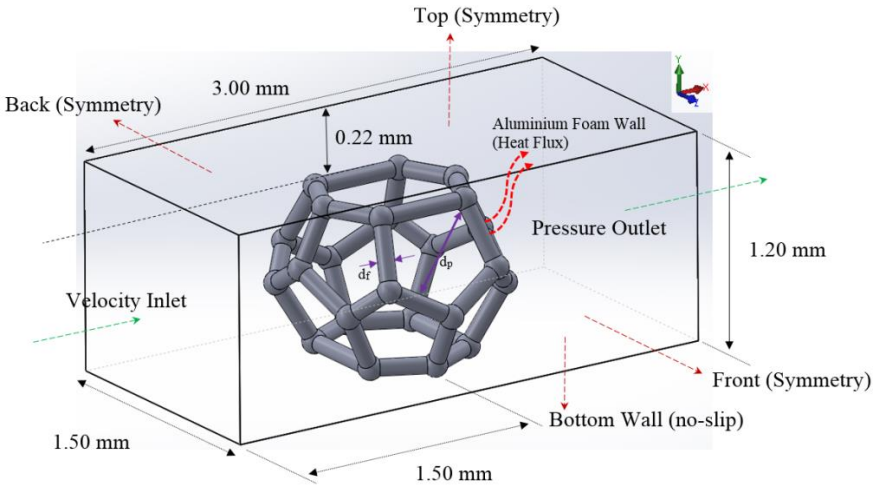

Fig.1 Computation domain of an idealized Weaire-Phelan unit cell and boundary conditions

A WP model is used in this investigation as it serves as a good representation of a real metal foam due to the significant presence of pentagonal faces, which is the norm in real metal foams[10]. The geometry is designed in SolidWorks. A no-slip wall is applied to the bottom face to simulate the bottom wall of a foam-filled pipe. The laminar gas coolant emanating

from the inlet is air at 300 K, and constant heat flux of 5 kW/m^2 [11] is imposed at the walls of the WP structure.

The finite volume method is used to discretise the equations on unstructured grids in general coordinates. The SIMPLE pressure-velocity coupling algorithm is deployed in the steady state numerical simulations. A second order upwind scheme is used for the momentum and energy spatial discretization. An under-relaxation factor of 0.7 and 1.0 is used for the momentum and energy terms respectively. The solution is initialized from the inlet at a known superficial inlet velocity, and the simulation is run until the convergence criteria for the residuals is reached.

The temperature profiles and interfacial heat transfer coefficient of the WP structures is numerically evaluated based on two inlet velocities, 0.25 m/s and 0.50 m/s. The morphological description of three metal foams presented in this study is shown in Table 2. It should be noted that the computation domain for Specimen 3 has dimensions 1.80 mm ×1.60 mm × 4.80 mm but the distance between the inlet and mid-section of a foam specimen is 1.50 mm for all three specimens (Fig.1).The cases presented in Table 1 will provide an insight into the effect of foam fibre thickness and foam porosity on the effective heat transfer performance of a metal foam specimen.

Table 1 Metal foam geometric profile

Metal foam	**Porosity, ε[%]**	**Average fibre diameter, d_f[mm]**	**Average pore diameter, $d_{p,avg}$ [mm]**
Specimen 1	97.79	0.09	0.61
Specimen 2	94.81	0.17	0.63
Specimen 3	97.87	0.17	0.63

A grid independent study is performed based on four different meshes to examine the dependence of the numerical pressure drop and temperature difference results based on specimen 1, as shown in Table 2. The simulation is set with an inlet velocity U_∞ of 0.50 m/s and a heat flux q of 5 kW/m^2 is imposed on the WP unit cell. A fine mesh is selected for the numerical analysis to reduce the computational cost.

Table 2 Mesh sensitivity analysis at U_∞ = 0.5 m/s and q = 5 kW/m^2

Mesh	**Nodes**	**Pressure Drop [Pa]**	**Maximum Temperature [K]**
Coarse	68,143	1.866	361
Medium	1,053,124	1.741	364
Fine	2,362,159	1.843	364
Very Fine	4,872,931	1.843	364

Results and Discussion

Heat Transfer Characteristics

The steady state temperature distribution profiles of the three metal foam specimens based on two superficial velocities is illustrated in Fig. 2.The temperature distribution profiles are sensitive to the ligament thickness, d_f. The maximum temperature is clearly observed in Specimen 3. All the foams exhibit lower temperature profiles at a higher superficial velocity due to a greater heat dissipation from the foam wall to the surroundings.

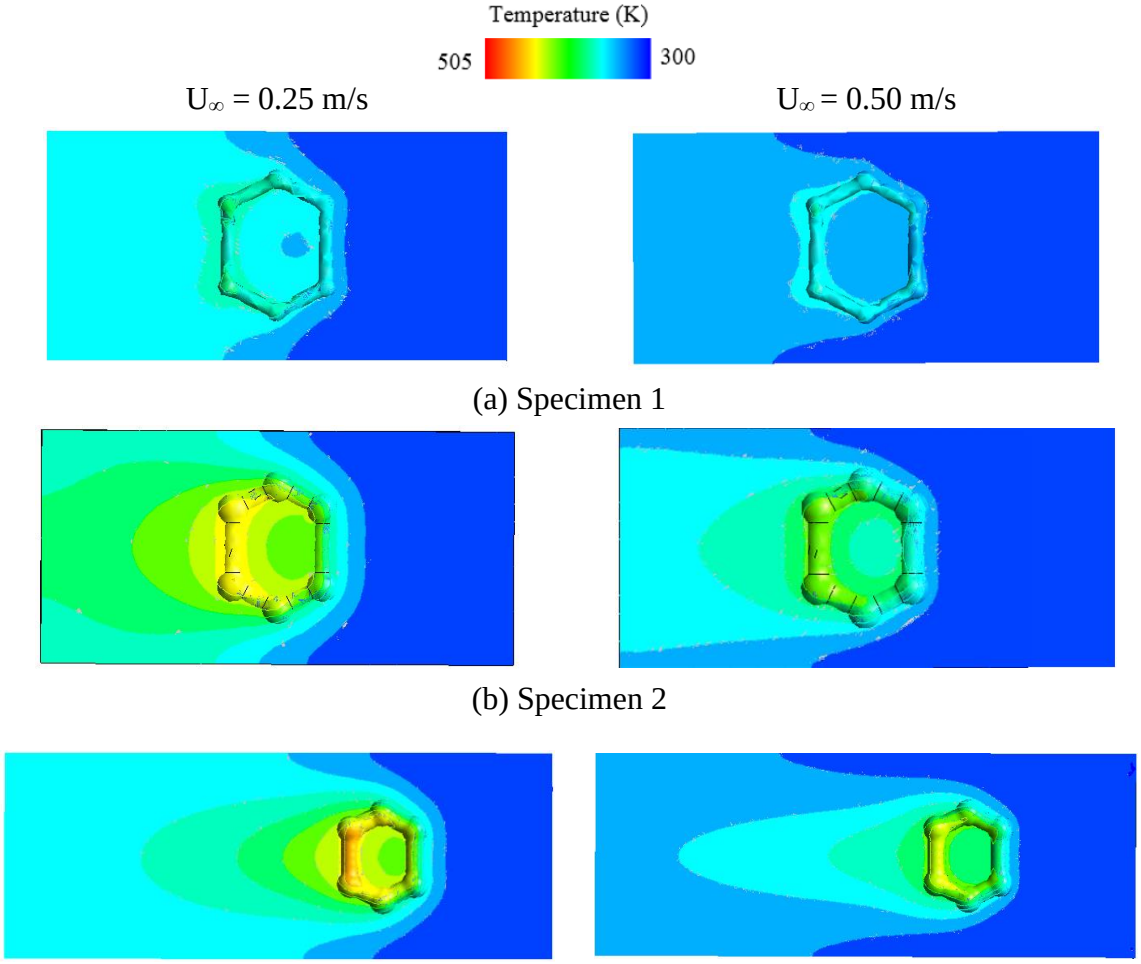

(a) Specimen 1

(b) Specimen 2

(c) Specimen 3

Fig. 2. Temperature distribution Weaire-Phelan (Bottom). Flow direction from right to left.

According to Tables 3 and 4, the highest temperature is realised in specimen 3, irrespective of the inlet velocity. The temperature (T_1 or T_2) and the maximum temperature difference (T_1-T_2) is more sensitive to the variation in foam fibre thickness than that of the foam porosity variation. For instance, Case B1 (identical porosity; different fibre thickness), exhibits a higher maximum temperature difference than Case C1 (different porosity; identical fibre thickness) by a factor of 6.13. The same conclusion is drawn between Cases A1/A2 and C1/C2. However, Case A1/A2 bothhaving different foam thickness and porosity, has a lower maximum temperature difference than Case B1/B2 by a factor of only 1.20. This shows that the fibre thickness plays a major role in the enhancement of the heat transfer performance.

Table 3 Comparison of metal foam maximum temperature distribution at U_∞ = 0.25 m/s

	Specimen (ε_1,$d_{f,1}$)	**T_1**	**Specimen (ε_2,$d_{f,2}$)**	**T_2**	**$\varepsilon_1 - \varepsilon_2$**	**$d_{f,1} - d_{f2}$**	**$T_1 - T_2$**
A1	Specimen 1 (97.79%, 0.09 mm)	380	Specimen 2 (94.81%, 0.17mm)	462	2.98	0.08	82
B1	Specimen 1 (97.79%, 0.09 mm)	380	Specimen 3 (97.87%, 0.17mm)	478	0.08	0.08	98
C1	Specimen 2 (94.81%, 0.17mm)	462	Specimen 3 (97.87%, 0.17mm)	478	3.06	0.00	16

Both Cases A and B show a difference in the maximum temperature distribution by about 30 %. Interestingly, an increase in the inlet velocity shows a negligible temperature difference between Cases C1 and C2. A significantly higher superficial velocity is thus required to dissipate the heat from the foam ligaments with higher thickness (0.17 mm).

Table 4 Comparison of metal foam maximum temperature distribution at U_∞ = 0.50 m/s

	Specimen (ε_1,$d_{f,1}$)	**T_1**	**Specimen (ε_2,$d_{f,2}$)**	**T_2**	**$\varepsilon_1 - \varepsilon_2$**	**$d_{f,1} - d_{f2}$**	**$T_1 - T_2$**
A2	Specimen 1 (97.79%, 0.09 mm)	364	Specimen 2 (94.81%, 0.17mm)	424	2.98	0.08	60
B2	Specimen 1 (97.79%, 0.09 mm)	364	Specimen 3 (97.87%, 0.17mm)	441	0.08	0.08	77
C2	Specimen 2 (94.81%, 0.17mm)	424	Specimen 3 (97.87%, 0.17mm)	441	3.06	0.00	17

Solid Particle Transport and Deposition

A preliminary investigation based on the transient pore-level isothermal particle-fluid transport and particle deposition of sandstone particles (2600 kg/m^3 density and 50 µm diameter) is conducted as shown in Fig.3. It should be noted that, this simulation is executed in OpenFOAM. The energy equations governing thermal transport of particle-fluid flows is currently not integrated in OpenFOAM. The authors aim to re-develop OpenFOAM's solver in the near future to account for the thermal interaction between fluid, particle, and the metal foam structure, all of which have different thermal conductivities.

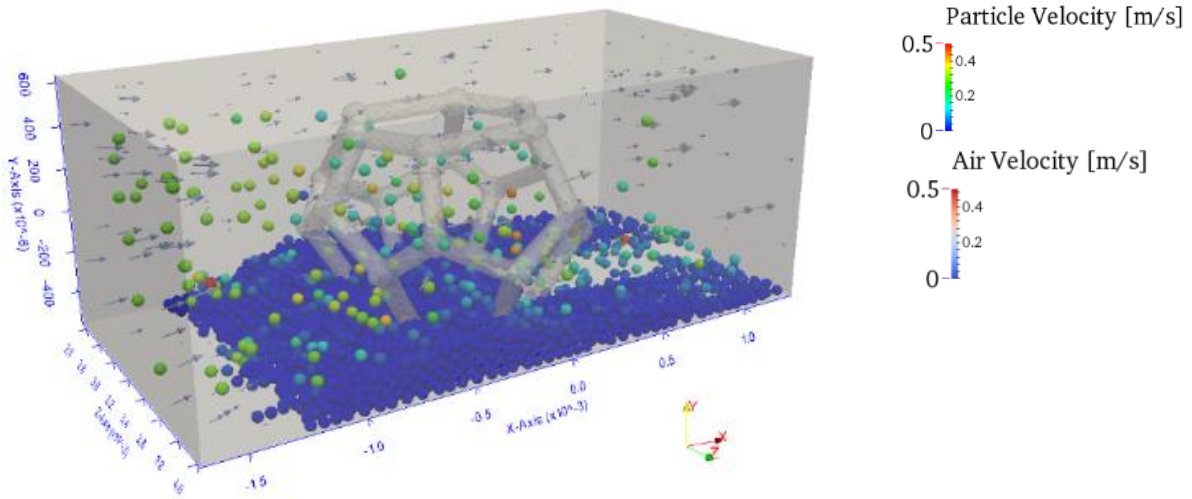

Fig.3 Particle deposition in Specimen 1 at end of simulation. Flow direction from left to right.

As can be seen in Fig. 3, a significant amount of particles have deposited at the bottom of the wall due to sedimentation and inertial impaction which acts as the primary mechanism of particle transport.By relating the result concerning particle deposition (Fig.3), with the results shown in Fig.2, the particle temperature profiles can be deduced by taking into account the *temperature hotspots* at the trailing edge of the metal foam (left hexagonal face) as shown in Fig.2. The trailing edge should see a large spread of particles with a high temperature, and a broader spread at 0.25 m/s. Particles with a high thermal conductivity such as copper dust, which is profound in mines, should accentuate the effective heat transfer performance of the foam whereas locations where saw dust with a significantly lower thermal conductivity could potentially mitigate the performance. Although certain particle deposits could potentially

enhance heat transfer performance, the pressure drop should theoretically increase. It may be possible to permit a certain amount of fouling to be immersed into a system to increase the overall heat transfer performance whilst having an acceptable pressure drop level.

Conclusions

A steady state numerical investigation of the heat transfer characteristics of three different idealized metal foams is conducted. Fibre thickness has a substantial influence on the overall heat transfer performance. The presence of fouling could either enhance or mitigate the effective heat transfer performance. Small traces of conductive foulant may be tolerable to enhance overall heat transfer performance. In the next step, the authors will develop a coupled finite volume and discrete element method (CFD-DEM) to account for the non-isothermal transport of discrete particles and fluid immersed in porous media.

References

[1] Acmite. (2013). *Global heat exchanger market report.* Tech. Rep..

[2] Han, X., Wang, Q., Park, Y., T'Joen, C., Sommers, A., & Jacobi, A. (2012). A review of metal foam and metal matrix composites for heat exchangers and heat sinks. *Heat Transfer Engineering, 33*(12), 991-1009.

[3] Hooman, K., & Gurgenci, H. (2011). Metal Foam Heat Exchangers for Heat Transfer Augmentation from a Tube Bank. *Applied Thermal Engineering, 36*(1), 456-463.

[4] Bai, M., & Chung, J. (2011). Analytical and numerical prediction of heat transfer and pressure drop in open-cell metal foams. *Int. J. of Thermal Sciences, 50*, 869-880.

[5] Huisseune, H., Schampheleire, S., Ameel, B., & Paepe, M. (2015). Comparison of metal foam heat exchangers to a finned heat exchanger for low Reynolds number applications. *International Journal of Heat and Mass Transfer, 89*, 1-9.

[6] Mahdi, H., Lopez, P., Fuentes, A., & Jones, R. (2006). Thermal performance of aluminium-foam CPU heat exchangers. *Int. J. of Energy Research, 30*(11), 851-860.

[7] Seyf, H.R., & Layeghi, M. (2010). Numerical analysis of convective heat transfer from an elliptic pin fin heat sink with and without metal foam insert. *J. of Heat Transfer, 132*(7), 1-9.

[8] Kuruneru, S., Sauret, E., Saha, S., & Gu, Y. (30 November – 01 December 2015). Poly-disperse particle transport and deposition in idealized porous channels. *Proceedings of the 2nd Australasian Conference on Comp. Mech. (ACCM2015).* Brisbane, Australia.

[9] Diani, A., Bodla, K., Rossetto, L., & Garimella, S. (2015). Numerical investigation of pressure drop and heat transfer through reconstructed metal foams and comparison against experiments. *International Journal of Heat and Mass Transfer, 88*, 508-515.

[10] Bock, J., & Jacobi, A. (2013). Geometric classification of open-cell metal foams using X-ray micro-computed tomography. *Materials Characterization, 75*, 35-43.

[11] Iasiello, M., Cunsolo, S., Oliviero, M., Harris, W., Bianco, N., & Chiu, W. &. (2014). Numerical analysis of heat transfer and pressure drop in metal foams for different morphological models. *Journal of Heat Transfer, 136*(11).